Electron Microscopy: Its Role in Materials Science (The Mike Meshii Symposium)
Edited by J.R. Weertman, M. Fine, K. Faber, W. King and P. Liaw TMS (The Minerals, Metals & Materials Society), 2003

TEMPORAL EVOLUTION OF NANOSTRUCTURES IN A MODEL NICKEL-BASE SUPERALLOY: EXPERIMENTS AND SIMULATIONS

Chantal K. Sudbrack[1], Kevin E. Yoon[1], Zugang Mao[1], Ronald D. Noebe[2], Dieter Isheim[1], and David N. Seidman[1]

[1]Northwestern University; Department of Materials Science and Engineering, 2220 Campus Drive; Evanston, IL 60208-3108 USA
[2] NASA Glenn Research Center; Cleveland, OH, 44135 USA

Abstract

The temporal evolution of the nanostructure of a model Ni-base superalloy (Ni-5.2 at.% Al-14.2 at.% Cr) is studied experimentally employing three-dimensional atom-probe (3DAP) microscopy in conjunction with kinetic Monte Carlo (KMC) simulations at 600°C. It is demonstrated that not only can the mean compositions of individual γ' (Ni_3Al with the $L1_2$ structure) precipitates be measured but the Ni, Al, and Cr concentration profiles within the precipitates can also be determined for precipitates with a mean radius (<r>) as small as 0.85 nm. The three asymptotic time dependencies of the Lifshitz-Slyzov-Wagner (LSW) theory of coarsening (Ostwald ripening) are measured and found to deviate from its theoretical predictions; possible explanations for these discrepancies are discussed. At 0.25 hr. there is 3DAP microscope evidence for the presence of precipitates of another nickel-rich phase, ≈"Ni_3Cr" ($Ni_3Cr_{1-x}Al_x$), which exhibits short-range order (SRO) and that is metastable with respect to Ni_3Al. This metastable phase is also found by KMC simulations and has the composition $Ni_3Cr_{1-x}Al_x$, which is Ni-2.91 at.% Al-21.98 at.% Cr at 16 hours. Our results demonstrate that the decomposition of the primary γ (FCC) phase results in the concurrent formation of an ordered phase and a disordered phase by 0.25 hours.

Introduction

The temporal evolution of a nano- or microstructure involves the nucleation, growth and coarsening of new phase(s), which is the result of the solid-state decomposition of an alloy at a specified aging temperature. The new phase(s) may be either metastable or equilibrium structures. This subject has been studied experimentally employing various experimental techniques [1,2,3], and theoretically utilizing diverse approaches [1,3,4,5]; including phase-field models [6] (encompassing the original Cahn-Hilliard treatment of the underlying diffusion equation), which are currently very popular [7,8], and kinetic Monte Carlo (KMC) simulations employing a vacancy mechanism for diffusion [9]. The nano- or microstructure of a material is of paramount importance as it determines its physical and mechanical properties, and the manipulation of a nano- or microstructure can be used for optimizing the desired properties.

The approaches we are utilizing to study the temporal evolution of nanostructures are different from the methods generally employed in that we combine atomic-scale experimental and simulation techniques, for similar numbers of atoms and length scales. The use of three-dimensional atom-probe (3DAP) microscopy, which provides three-dimensional real space images with atom-by-atom chemical information, in concert with KMC simulations yields a nearly complete atomistic picture. This is particularly useful for studying the effects of short-

range order and clustering phenomena. In addition electron microscopies are used to complement and supplement these methods.

Nickel-base superalloys for high-temperature utility gas turbine [10] and aviation turbine [11] blades is a highly sophisticated subject that has been evolving continuously for more than 25 years. Its application to aviation turbine blades has progressed from the use of equiaxed grain structures to directionally solidified grain-structures and currently to single-crystal blades, which are two-phase γ/γ'(FCC/$L1_2$) structures, containing as many as 12 alloying elements. The current generation of Ni-base superalloys, e.g., CMSX-10M and René N6, have evolved from earlier generations and their design has utilized this γ/γ' system and the effects of alloying elements on the high-temperature physical and mechanical properties. Also the sign of the γ/γ' lattice parameter mismatch plays a significant role on the elevated temperature creep strength, in particular a mismatch of zero improves the creep properties by preventing the evolution of a γ'-rafted morphology [12].

We present some results for a model nickel-base superalloy, Ni-5.2 at.% Al-14.2 at.% Cr, which is close to the composition studied earlier by Schmuck et al. [13], whose nanostructure is allowed to evolve temporally at 600°C. The principal experimental tool utilized is 3DAP microscopy. The experimental measurement of the three asymptotic time ($t \rightarrow \infty$) dependencies predicted by the Lifshitz-Slyzov-Wagner (LSW) coarsening (Ostwald ripening) model [14,15,16,17] are shown to exhibit deviations from the predicted values. In addition, we present 3DAP microscopy evidence for a metastable phase, ≈"Ni_3Cr" ($Ni_3Cr_{1-x}Al_x$), that co-exists with Ni_3Al at 0.25 hr., thereby demonstrating that decomposition and ordering are occurring concurrently.

Three-Dimensional Atom-Probe (3DAP) Microscope Experimental Results

First, homogenization of bulk specimens is performed at 1300°C for 20 hours, followed by a vacancy equilibration treatment for 3 hours at 850°C in the single-phase region. Finally, the specimens are aged at 600°C for 0, 0.25, 1, 4, 16, 64 or 256 hrs. and water quenched, which results in the decomposition of this alloy into the γ(FCC) and γ' ($L1_2$ structure) phases. Figure 1 exhibits 10x10x25 nm^3 subsets of the 3DAP reconstructions of volumes of this alloy aged at 600°C, created employing *ADAM 1.5* [18], at the indicated aging times. Each rectangular parallelepiped contains 130,000 atoms, which are omitted for the sake of clarity. The Ni_3Al precipitates are delineated by a 9 at.% Al gray isoconcentration surface, which aids in visualizing the temporal evolution of the Ni_3Al precipitates (γ'-phase). Note that after aging for 0.25 hr. the Ni_3Al precipitates are clearly visible and they have a mean radius, <r>, of 0.85

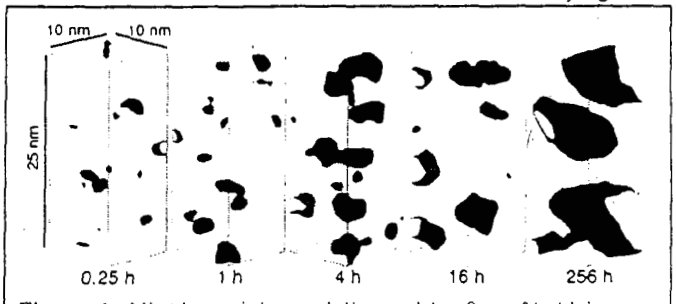

Figure 1: Ni_3Al precipitates delineated by 9 at. % Al isoconcentration surfaces in Ni-5.24 Al-14.24 Cr at. % samples aged at 600°C, for a series of aging times, revealing the temporal evolution of the nanostructure. Each volume, 10 x 10 x 25 nm^3 in size and containing approximately 130,000 atoms, is a subset of the experimentally obtained 3DAP reconstructions; the individual atoms are not exhibited for the sake of clarity.

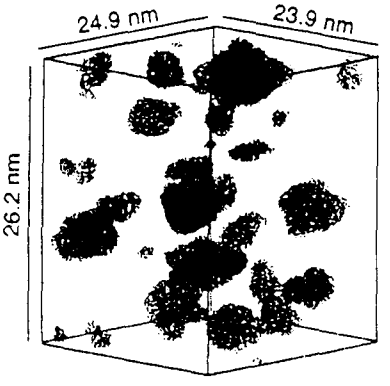

Figure 2: 3DAP reconstruction of Ni-5.24 Al-14.24 Cr (at. %) aged at 600°C for 16 h, where all atoms, 49,437 Ni, Al, and Cr atoms, within a 9 at. % Al isoconcentration surface are displayed. Utilizing our analysis program, *ADAM 1.5*, individual precipitates are clearly detected and delineated. The volume contains 724,442 atoms in total but only the ones in the Ni_3Al precipitates are shown for clarity.

nm (Fig. 3); it is clear that this system coarsens with increasing time. Figure 2 is a 3DAP reconstruction, after aging at 600°C for 16 h, where all the atoms within a 9 at.% Al isoconcentration surface are displayed. We are therefore able to extract the properties of *individual* precipitates, for example, composition, radius, degree of order, approximate morphology, etc.. Figure 3 exhibits average radial composition profiles for γ' precipitates after aging for different times at 600°C; these profiles are created from the indicated numbers of precipitates and are centered on each precipitate. Note that <r> of the γ' precipitates increases with increasing aging time -- from 0.85, to 1.44, to 1.92 nm -- as time increases from 0.25 hr. to 64 hrs. . Additionally, Fig. 3 demonstrates that the composition profiles of Ni, Al and Cr within the precipitates are changing with increasing time during coarsening, which implies that the γ' precipitates have a composition that is time dependent. Particularly, note that the maximum concentration of Al at the precipitate center diminishes with increasing aging time. The upper panel in Fig. 4 displays the number density (N_v) and the lower panel <r> of the $Ni_3Cr_{1-x}Al_x$ as a function of aging time at 600°C; also note the data of Schmuck et al. [13]. Firstly, the initial slope of the N_v vs. time plot is 0.10±0.05 (our data) and the final slope becomes –0.75±0.15 after four hrs., which is the same as observed by Schmuck et al.; the latter regime involves coarsening. Also the initial slope of the <r> vs. aging time (0.25 to 1 hr.) graph is approximately zero and becomes 0.27 (our data) after 1 hr, while the Schmuck et al. data has a slope of 0.23 commencing with 4 hours. Finally, Fig. 5 is a double logarithmic plot, to the base 10, of the supersaturation vs. time for both Al and Cr, which yields values for the exponent of time. The experimental values are equal to –0.23 and –0.25 for Al and Cr, respectively, while the KMC values are –0.31 for Al and –0.25 for Cr. To obtain the concentrations at infinite time we plotted the Cr or Al concentrations away from the γ/γ' interfaces as a function of $(t)^{-1/3}$. Between 0.25 and 1 hr. there is a transient, which is followed by a regime of constant slope. The concentration values extrapolated to infinite

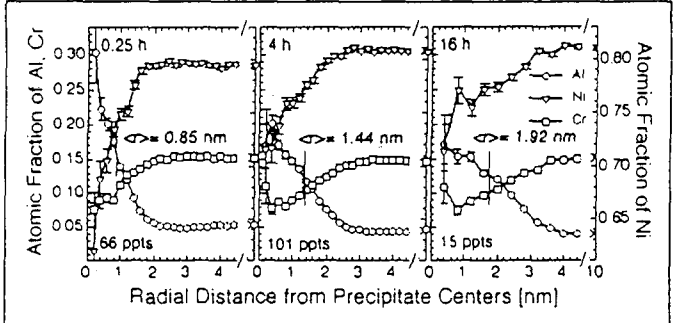

Figure 3: Average radial composition profile from the precipitate centers as a function of time in Ni-5.24 Al-14.24 Cr at. % aged at 600°C. Note that the mean radius, <r>, is increasing with increasing time from 0.25 hr. to 16 hrs.

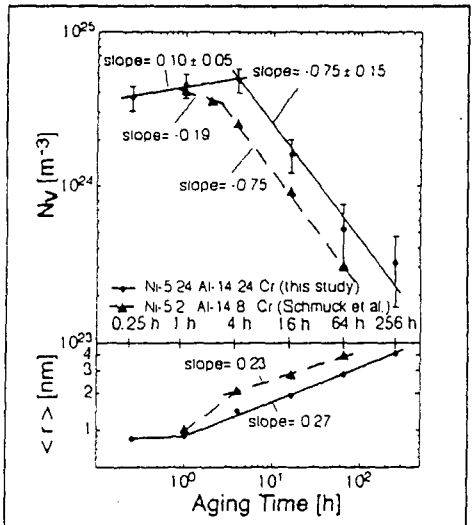

Figure 4: The temporal evolution of the Ni_3Al precipitate number density (*top*) and mean precipitate radius (*bottom*) in Ni-5.24 Al- 14.24 Cr at. % aged at 600°C.

time ($t^{-1/3}$ = 0), correspond to the solid-solubilities (2.98 Al, 15.64 Cr at.%) in the γ (FCC) phase.

Theoretically for a ternary alloy the asymptotic solutions ($t \rightarrow \infty$) define the steady state in the LSW coarsening model, which predict that N_v is proportional to $(t)^{-1}$, <r> is proportional to $(t)^{1/3}$, and the supersaturation is proportional to $(t)^{-1/3}$ [19]. The supersaturation is defined to be the time-dependent concentration of a solute species in the matrix, Al and Cr in this case, far from the matrix/precipitate interface (γ/γ'), minus its thermodynamic equilibrium concentration in the matrix (i.e., the value of the concentration in the matrix as $t \rightarrow \infty$). Our 3DAP microscopy experiments unequivocally demonstrate that the three exponents differ from the *exact* values predicted by LSW theory, and hence the physical assumptions of the highly idealized LSW model for coarsening are *not* exactly fulfilled. Therefore, the evolution of this γ/γ' system is not in steady-state as defined by the three asymptotic time dependencies of LSW theory, as experimentally demonstrated by the data presented in Figs. 4 and 5. We are perhaps observing the effects of transient coarsening, and/or the overlap of diffusional fields [20], and/or effects associated with the asymmetric mobility properties of vacancies in the γ and γ' phases [21], and/or the fact that the concentrations within the γ' precipitates are not a constant as assumed by LSW theory. The precise origins of the observed discrepancies remain to be clarified in the future. These results demonstrate that all three time-dependencies can be determined experimentally employing this direct approach for a ternary alloy [22,23], which is possible because of the unique capability of the 3DAP microscope to determine chemistry on a sub- to nanoscale. Also the 3DAP microscope allows one to obtain data sets that are statistically significant. Note that the slopes calculated by KMC simulations are also less than -1/3 (Fig. 5.)

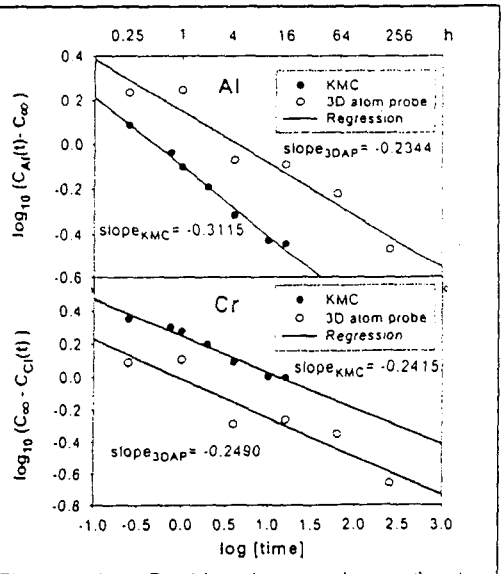

Figure 5: Double $\log_{10}$ plot of the supersaturation versus time (hr.); see text for the definition of supersaturation employed. Comparison of the experimental values (3DAP microscopy) with the kinetic MC values for a Ni-5.24 Al-14.24 Cr at.% alloy aged at 600°C.

Finally, Figs 3 and 6 demonstrate that at 0.25 hr. Ni_3Al and ≈"Ni_3Cr" ($Ni_3Cr_{1-x}Al_x$)

precipitates co-exist with one another. A detailed analysis of the chemistry of the ≈"Ni_3Cr" ($Ni_3Cr_{1-x}Al_x$) precipitates along a <001> direction indicates the presence of alternating pure Ni and mixed Ni-Cr planes (see inset in Fig. 6), which is characteristic of the $L1_2$ structure. We note, however, that we do not yet have diffraction evidence for the exact crystal structure of this phase. A combined proxigram concentration profile [24] (*lower right* of Fig. 6) of two 3DAP analyses (1.5 million atoms) exhibits a Cr concentration close to 40 at.% at the center of the precipitates. These results represent direct experimental evidence for the existence of two ordered phases ≈"Ni_3Cr" ($Ni_3Cr_{1-x}Al_x$) and Ni_3Al and therefore both phase separation and ordering are occurring in parallel in this alloy with ≈"Ni_3Cr" appearing to be metastable with respect to Ni_3Al; further details are to be published. The lowest temperature Taylor and Floyd [25] studied the Ni-Cr-Al phase diagram was 750°C and hence there is not an experimentally determined phase diagram at 600°C in the pertinent region to compare with.

Kinetic Monte Carlo Simulation Results

The experimental ternary Ni-Al-Cr phase diagram has only been studied to a certain degree as a function of temperature and composition [25,26]. It can, however, be simulated employing grand canonical ensemble MC (GCEMC) simulations and Pareige et al. used this approach to calculate the Ni-Al-Cr ternary phase diagram at 600°C [27]. Their results agree with the existing ternary phase diagram, which was extrapolated from 750°C to 600°C, thus demonstrating that their interatomic energy parameters correctly capture the thermodynamics of this ternary alloy.

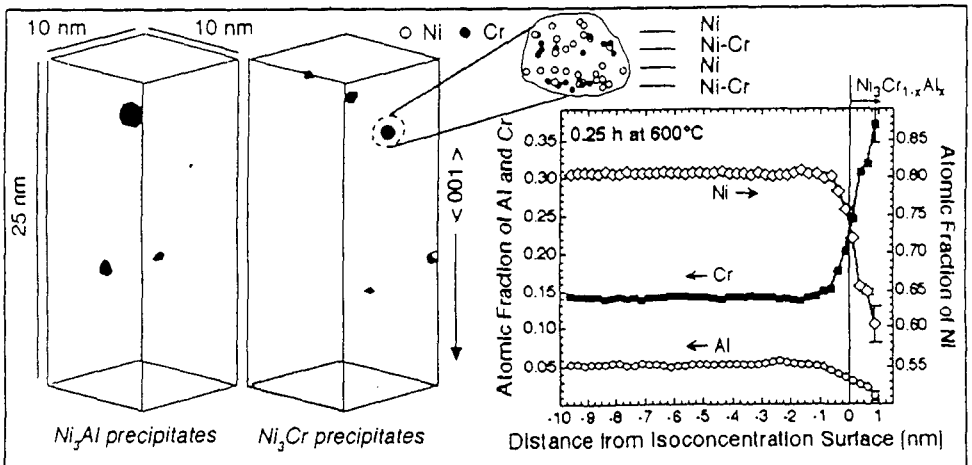

Figure 6: The 10 x 10 x 25 nm^3 subset (containing approximately 130,000 atoms) of a 3DAP reconstructed volume, analyzed along the 001 pole using 3DAP microscopy, of Ni-5.24 Al-14.24 Cr at. % aged for 0.25 h at 600°C shows evidence for both Ni_3Al and ≈"Ni_3Cr" precipitation (*left*). The Ni_3Al and ≈ "Ni_3Cr" ($Ni_3Cr_{1-x}Al_x$) precipitates are discerned using 9 at. % of Al and 17.5 at. % of Cr isoconcentration surfaces. Examination of the atoms within one precipitate within the volume reveals alternating pure Ni and mixed Ni-Cr planes along a <001>, direction characteristic of the ordered $L1_2$ crystal structure (*upper right*). Utilizing 17.5 at. % Cr isoconcentration surface, the combined proxigram concentration profile of two 3DAP analyses, totaling 1.5 million atoms, shows Cr enrichment with a maximum at ~40 % Cr within the center of the precipitates (*lower right*).

We have independently simulated the Ni-Al-Cr phase diagram at 600°C, 750°C and 800°C using the GCEMC approach with the same interatomic energy parameters as those employed by Pareige et al. . Our simulated phase diagrams are displayed in Fig. 7 and are in reasonable agreement with the existing experimental ternary phase diagram at 750°C, for the regions we have explored to date, extrapolated from 750°C to 600°C and to 800°C. This simulation of the Ni-Al-Cr phase diagram constitutes an important and basic test of the interatomic energy parameters for calculating thermodynamic quantities.

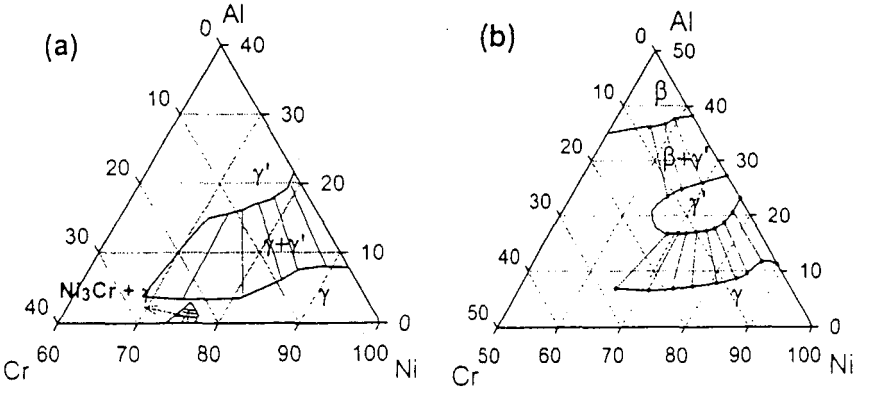

Figure 7: Grand canonical ensemble Monte Carlo (GCEMC) simulation of partial Ni-Cr-Al phase diagrams at (a) 600 °C and (b) 800°C. Note the presence of the phase field containing $Ni_3Cr_{1-x}Al_x$ plus γ at 600°C.

In addition, we have simulated the temporal evolution of the γ'-phase ($L1_2$ structure) as a function of aging time at 600°C, for 0.25, 1, 4 and 16 hrs. and find that $Ni_3Cr_{1-x}Al_x$ precipitates appear initially followed by Ni_3Al. The mechanism involves the substitution of Al atoms for Cr atoms in $Ni_3Cr_{1-x}Al_x$, so that the $Ni_3Cr_{1-x}Al_x$ precipitates appear to be continuously transforming to Ni_3Al (γ'-phase); this point is being further investigated using both the 3DAP microscope and KMC simulations. After 16 hr. the mean composition of these precipitates is Ni-2.91 at.% Al-21.98 at.% Cr. We also observe the "piggy back" nucleation of Ni_3Al precipitates on $Ni_3Cr_{1-x}Al_x$ precipitates creating a $Ni_3Al/Ni_3Cr_{1-x}Al_x$ interface. The KMC simulation results taken in concert with the 3DAP microscope results provide convincing evidence for the existence of metastable $Ni_3Cr_{1-x}Al_x$ precipitates at 600°C, which exhibit short range order.

Conclusions

We have studied the temporal evolution of the nanostructure of a model nickel-base superalloy (Ni-5.2 at.% Al-14.2 at.% Cr) at 600°C, employing three-dimensional atom-probe microscopy and kinetic Monte Carlo simulations. The decomposition of the γ (FCC) phase results in the initial appearance of a metastable phase, $Ni_3Cr_{1-x}Al_x$, which exhibits short-range order. This phase is detected in both the 3DAP microscope experiments and the kinetic Monte Carlo simulations. The three asymptotic ($t \rightarrow \infty$) temporal dependencies of the LSW theory of coarsening of the γ' ($L1_2$ structure) precipitates are measured and found to deviate from all three predicted values; possible reasons for this result are discussed. It is demonstrated that not only can the mean composition of individual precipitates be measured but the radial composition profiles of the elements Ni, Al and Cr within the precipitates can be determined and followed temporally for precipitates with radii as small as 0.85 nm.

Acknowledgements

This research is sponsored by the National Science Foundation (Dr. K. L. Murty, grant officer). KEY is partially supported by a NASA GSRP Fellowship, CKS is partially supported by an NSF fellowship, and Dr. Ronald D. Noebe acknowledges support from the NASA Glenn HOTPC program. Professor Pascal Bellon (University of Illinois at Urbana-Champaign) is kindly thanked for his generous help and advice concerning the kinetic Monte Carlo simulations.

References

1. G. Martin, "The Theories of Unmixing Kinetics of Solid Solutions," in: D. de Fontaine, Editor, Solid State Phase Transformations in Metals and Alloys (Orsay, France: Les Editions de Physique, 1978), pp. 337-406.
2. R. Kampmann and R. Wagner, "Kinetics of Precipitation in Metastable Binary Alloys: Theory and Application to Cu-1.9 at.% Ti and Ni-14 at.% Al," in: P. Haasen, Editor, Decomposition of Alloys, the Early Stages: Proceedings of 2nd Acta-Scripta Metallurgica Conference (Oxford, Great Britain: Pergamon, 1983), pp. 912-103.
3. R. Wagner, R. Kampmann and P. W. Voorhees, "Homogeneous second-phase precipitation", in: G. Kostorz, Editor, Phase Transformations in Materials (Weinheim, Germany: Wiley-VCH, 2001), pp. 309 – 408.
4. A. G. Katchaturyan, Theory of Structural Transformations in Solids (New York, NY: John Wiley, 1983).
5. W. A. Soffa and D. E. Laughlin, "Decomposition and Ordering Processes Involving Thermodynamically First-Order Transformations," Acta Metallurgica, 37 (1989) 3019-3028.
6. A. G. Katchaturyan, T. F. Lindsey, and J. W. Morris, "Theoretical Investigation of the Precipitation of δ' in Al-Li," Metallurgical Trans., 19A (1988) 249-258.
7. Long-Qing Chen, "Phase-Field Models for Microstructure Evolution," Annu. Rev. Materials, 32 (2002) 113-140.
8. D. Fan, S. P. Chen, Long-Qing Chen, and P. W. Voorhees, "Phase-Field Simulation of 2-D Ostwald Ripening in the High Volume Fraction Regime," Acta Materialia, 50 (2002) 1895-1907.
9. T. A. Abinandanan, F. Haider, and G. Martin, "Computer Simulations of Diffusional Phase Transformations: Monte Carlo Algorithm and Application to Precipitation of Ordered Phases," Acta Materialia, 46 (1998) 4243-4255.
10. B. B. Seth,"Superalloys – The Utility Gas Turbine Perspective," in Superalloys 2000, Editors, T. M. Pollock, R. D. Kissinger, R. R. Bowman, K. A. Green, M. McLean, S. L. Olson, J. J. Schirra (Warrendale, PA: TMS-The Minerals, Metals, & Materials Society, 2000), pp. 23-16.
11. C. T. Sims, in Superalloys II High-Temperature Materials for Aerospace and Industrial Power, Editors, C. T. Sims, N. S. Stoloff, and W. C. Hagel (New York: John Wiley & Sons Inc., 1987), Chap. 1.
12. R. A. MacKay, M. V. Nathal, and D. D. Pearson, "Influence of Molybdenum on the Creep Properties of Nickel-Base Superalloy Single Crystals," Metallurgical Transactions, 21A (1990) 381-388.

13. C. Schmuck, P. Caron, A. Hauet, and D. Blavette, "Ordering and Precipitation of γ' Phase in Low Supersaturated Ni-Cr-Al Model Alloy: An Atomic Scale Investigation," Philosophical Magazine A, 76 (1997) 527-542.
14. I. M. Lifshitz and V. V. Slyozov, "The Kinetics of Precipitation from Supersaturated Solid-Solutions," *J. Phys. Chem. Solids*, **19**, 35-50 (1961).
15. C. Wagner, "Theorie der altering von niederschlägen durch umlösen (Ostwald-reifung)," Z. Elektrochemie, **65**, 581-591 (1961).
16. I. Rubenstein and B. Saltzman, "Diffusional Mechanism of Coarsening in Ostwald Ripening," Physical Review E, 61 709-717 (2000) 709-717.
17. L. Ratke and P. W. Voorhees, Growth and Coarsening (Berlin, Germany: Springer Verlag, 2002), Chap. 8, p. 165.
18. O.C. Hellman, J. A. Vandenbroucke, J. Blatz du Rivage and D. N. Seidman, "Application Software for Data Analysis for Three-Dimensional Atom-Probe Microscopy," Materials Science & Engineering A, 327 (2002) 29-33.
19. C. J. Kuehmann and P. W. Voorhees, "Ostwald Ripening in Ternary Alloys," Metallurgical and Materials Transactions A, 27A (1996) 937-943.
20. M. K. Chen and P. W. Voorhees, "The Dynamics of Transient Ostwald Ripening," Modeling Simulation Materials Science & Engineering 1 (1993) 591-612.
21. J.-M. Roussel and P. Bellon, "Vacancy-Assisted Phase Separation with Asymmetric Atomic Mobility: Coarsening Rates, Precipitate Composition, and Morphology,' Physical Review B, 63 (2001) 184114-1-184114-15.
22. D. J. Chellman and A. J. Ardell, "The Effect of Volume Fraction on Particle Coarsening," Acta Metallurgica, 22 (1974) 577-588.
23. M. Fährmann, E. Fährmann, T. M. Pollock, and W. C. Johnson, "Element Partitioning During Coarsening of (γ–γ') Ni-Al-Mo alloys," Metallurgical and Materials A, 28A. (1997) 1943-1945.
24. O. C. Hellman, J. A. Vandenbroucke, J. Rüsing, D. Isheim, and D. N. Seidman, "Analysis of Three-Dimensional Atom-Probe Data by the Proximity Histogram," Microscopy and Microanalysis, 6 (2000) 437-444.
25. A. Taylor and R. W. Floyd, "The Constitution of Nickel-Rich Alloys of the Nickel-Chromium-Aluminum System,' Journal Institute Metals, 81 (1952-53) 451-464 .
26. M. F. Singleton, J. L. Murray, and P. Nash, in Binary Alloy Phase Diagrams, Editors, T. B. Massalski, J. L. Murray, L. H. Bennett, and H. Baker, (Metals Park, OH: ASM, 1986).
27. C. Pareige, F. Soisson, G. Martin and D. Blavette, "Ordering and Phase Separation in Ni-Cr-Al: Monte Carlo Simulations vs. Three-Dimensional Atom Probe," Acta Materialia, 47 (1999) 1889-1899.